

## Photodouble ionization of He with circularly polarized synchrotron radiation: complete experiment and dynamic nodes

This article has been downloaded from IOPscience. Please scroll down to see the full text article.

2008 J. Phys. B: At. Mol. Opt. Phys. 41 051003

(<http://iopscience.iop.org/0953-4075/41/5/051003>)

View [the table of contents for this issue](#), or go to the [journal homepage](#) for more

Download details:

IP Address: 38.107.179.214

The article was downloaded on 22/02/2012 at 07:08

Please note that [terms and conditions apply](#).

## FAST TRACK COMMUNICATION

# Photodouble ionization of He with circularly polarized synchrotron radiation: complete experiment and dynamic nodes

P Bolognesi<sup>1</sup>, V Feyer<sup>1</sup>, A Kheifets<sup>2</sup>, S Turchini<sup>3</sup>, T Proserpi<sup>3</sup>, N Zema<sup>3</sup>  
and L Avaldi<sup>1,4</sup>

<sup>1</sup> CNR-IMIP, Area della Ricerca di Roma 1, 00016 Monterotondo Scalo, Italy

<sup>2</sup> Research School of Physical Sciences and Engineering, ANU, Canberra, Australia

<sup>3</sup> CNR-ISM, Area della Ricerca di Roma 2, Via Fosso del Cavaliere, Roma, Italy

<sup>4</sup> CNR-INFN-TASC, Gas Phase Photoemission Beamline@Elettra, Trieste, Italy

Received 22 January 2008, in final form 1 February 2008

Published 26 February 2008

Online at [stacks.iop.org/JPhysB/41/051003](http://stacks.iop.org/JPhysB/41/051003)

## Abstract

The combination of measurements of the photodouble ionization (PDI) of He with linearly and circularly polarized synchrotron radiation has allowed to obtain experimentally the moduli and relative phase of the complex amplitudes needed for the complete description of the process. The same quantities have been used to calculate other observables of the process (linear dichroism, asymmetry parameter of the angular distribution of one of the two photoelectrons and He<sup>2+</sup> recoil momentum distribution). Moreover, the present measurements prove definitely the existence of the dynamic nodes predicted by theories in the circular dichroism of PDI and associate them to a reduction of dimensionality of the process.

(Some figures in this article are in colour only in the electronic version)

The understanding of the correlated motion of electron pairs is of fundamental interest for the knowledge of the structure and properties of matter. In the last ten years it has been proved that the study of photodouble ionization, PDI, of He, the simplest process dominated by electron correlations, can provide valuable and unique information on this topic [1]. The deepest understanding of PDI is achieved in coincidence experiments where either the two photoelectrons or a photoelectron and the recoiling ion are detected. In these experiments the triple differential cross section,  $d^3\sigma/d\Omega_1 d\Omega_2 dE_1$  (TDCS) is measured.  $\Omega_1 = (\theta_1, \varphi_1)$  and  $\Omega_2 = (\theta_2, \varphi_2)$  are the angles of emission of the two electrons and  $E_1$  is the energy of one of them. The energy of the second electron is determined by energy conservation  $h\nu - IP^{2+} = E_1 + E_2$ , where  $h\nu$  is the photon energy and  $IP^{2+}$  the double ionization potential. By considering the <sup>1</sup>P<sup>o</sup> symmetry of the electron pair continuum wavefunction and

the invariance by rotation about a preferential symmetry axis, the full separation of the geometrical factors and the dynamic parameters in the TDCS is achieved [2]. The formers come from the description of the photon–atom interaction in the dipole approximation; the latter include all the information on the dynamics of the process in two complex amplitudes  $a_g(E_1, E_2, \theta_{12})$  and  $a_u(E_1, E_2, \theta_{12})$  [2], symmetric (gerade) and antisymmetric (ungerade), respectively, in the exchange of the two electrons. These basic quantities, calculated by the theories, are used to reconstruct any particular TDCS. The extraction of the moduli and relative phase,  $\delta$ , of the amplitudes from experiments is of considerable interest, because it allows a direct comparison among different sets of data and between theory and experiment. After some attempts relying upon parametrizations with various degree of complexity and approximation [3, 4], Bolognesi *et al* [5] proposed a procedure that (i) does not rely on any approximation, (ii)

needs only three determinations of the TDCS at the same relative angle  $\theta_{12}$  between the photoelectrons and (iii) can be applied to any set of experimental data. The method, applied to measurements with linearly polarized incident radiation, provides  $|a_g|^2$ ,  $|a_u|^2$  and  $\cos \delta$  [5], while the sign of  $\delta$  remains undetermined. When two sets of measurements at the same  $h\nu$ ,  $E_1$  and  $E_2$  with linearly and circularly polarized radiation are combined then also the sign of  $\delta$  is determined and the complete description of the process achieved. The He TDCS measured with circularly polarized radiation display a helicity dependence, i.e. a non-vanishing circular dichroism, CD [6, 7]. The observation of chirality in an electron pair ejected by a target with a spherically symmetric ground state ( $^1S_e$ ) might surprise, because in the common wisdom chirality is associated with objects not identical to their mirror image. However Berakdar and Klar [6] showed that, due to parity conservation, the helicity of the incident photon is transferred to the three body-system, the He atom, and the continuum spectrum of this excited system depends on the helicity of the absorbed photon. CD is proportional to  $\sin \delta$  [1]. Thus the combination of the CD measurement and three TDCS measured with linearly polarized radiation provides the full information for a complete experiment [5]. Another procedure [8], based on COLTRIMS experiments, can provide analogous results [9]. However the four experimental geometries needed in that procedure are not achieved by most of the set-ups used in PDI experiments. By contrast our procedure can be applied with no restrictions to any set of experimental data.

The first calculations of CD in He [7] predicted that for certain values of  $E_1 + E_2$ ,  $R = E_2/E_1$  and  $\theta_{12}$ , CD can vanish in a non-trivial way, i.e. due to the vanishing neither of the amplitudes nor of the geometrical factors. Later calculations in the convergent close coupling, CCC, model [10] and recently in the lowest-order perturbative approach [11] supported this result. Some experiments (see table 1 in [1]) provided an indirect evidence of these ‘dynamic nodes’, while a recent measurement at  $E_1 + E_2 = 60$  eV and  $R = 5$  and 11, supported by the predictions of the hyperspherical  $R$  matrix with semiclassical outgoing wave model, did not display such nodes [12].

The aim of this work is twofold: (i) to achieve a complete description of the PDI process via measurements with linearly and circularly polarized radiation and (ii) to prove definitely the existence of the dynamic nodes.

The experiments have been done with the multicoincidence end-station [13] at the GAPH [14] and CIPO [15] beamlines of the Elettra storage ring. The two rotatable turntables of the end-station host ten electrostatic hemispherical analyzers in the plane perpendicular to the direction,  $z$ , of the incident radiation. The three analyzers of the smaller turntable have been set to detect low energy electrons ( $E_1 = 3.5$  eV), while the other seven detect electrons with  $20 \leq E_2 \leq 50$  eV depending on the measurement. The set-up and experimental procedure have been described elsewhere [13].

The light source of the GAPH beamline is an undulator which provides completely linearly polarized radiation. The light source of the CIPO beamline is an electromagnetic

elliptical undulator/wiggler, which provides radiation of variable polarization state. In the energy range of interest the radiation is characterized by Stoke parameters  $S_1 = 0.24$ ,  $S_3 = \pm 0.97$  ( $S_3 > 0$  corresponds to a radiation whose polarization vector rotates clockwise for an observer looking towards the source) and the major axis of the polarization ellipse lays at  $\lambda = \pm 34^\circ$  for  $S_3 = \pm 0.97$ , respectively, with respect to the orbital plane of the electrons in the ring [15].

In the case of elliptically polarized radiation, the TDCS in the plane perpendicular to the direction of the radiation can be expressed as [12]

$$\begin{aligned} \text{TDCS}(E_1, E_2, \theta_{12}) = & \{|a_g|^2(1 + \cos \theta_{12}) + |a_u|^2(1 - \cos \theta_{12})\} \\ & + S_1 \{\cos(2\theta_1 + \theta_{12})[|a_g|^2(1 + \cos \theta_{12}) \\ & - |a_u|^2(1 - \cos \theta_{12})] + 2 \sin(2\theta_1 + \theta_{12}) \sin \theta_{12} \text{Re}(a_g a_u^*)\} \\ & - 2S_3 \sin \theta_{12} \text{Im}(a_g a_u^*), \end{aligned} \quad (1)$$

where  $\vartheta_1$  is referred to the major axis of the polarization ellipse and  $\theta_{12}$  is the relative angle between the two photoelectrons. The reduction of TDCS in equation (1) to the case of fully linearly polarized radiation ( $S_1 = 1$ ,  $S_3 = 0$ ) is straightforward [1]. The circular dichroism, CD, which is obtained by the TDCS measured with radiation of both helicities, is defined by

$$\begin{aligned} \text{CD}(E_1, E_2, \theta_{12}) &= \frac{1}{|S_3|} [\text{TDCS}_L(E_1, E_2, \theta_{12}) - \text{TDCS}_R(E_1, E_2, \theta_{12})] \\ &= -4 \sin \vartheta_{12} |a_g| |a_u| \sin \delta, \end{aligned} \quad (2)$$

where  $\text{TDCS}_L$  ( $\text{TDCS}_R$ ) is the TDCS for PDI by left (right), i.e.  $S_3 = -1(+1)$ , circularly polarized radiation. From the experimental point of view it is convenient to define the normalized circular dichroism,  $\text{CD}_n$ ,

$$\begin{aligned} \text{CD}_n(E_1, E_2, \theta_{12}) &= \frac{\text{TDCS}_L(E_1, E_2, \theta_{12}) - \text{TDCS}_R(E_1, E_2, \theta_{12})}{\text{TDCS}_L(E_1, E_2, \theta_{12}) + \text{TDCS}_R(E_1, E_2, \theta_{12})} \end{aligned} \quad (3)$$

equations (1)–(3) and the procedure described in [5] show that measurements with linearly and circularly polarized radiation provide the full information on the complex amplitudes, i.e. their moduli and relative phase.

Three TDCS measured at  $h\nu = 127$  eV for  $E_1 = 3.5$  eV,  $E_2 = 44.5$  eV,  $S_1 = 1$  and  $\theta_1 = 0^\circ, 30^\circ$  and  $60^\circ$  are shown in figure 1(a)–(c). The experimental data have been compared with the predictions of the CCC model [10]. The three TDCS of figure 1(a)–(c), being measured simultaneously, are on the same relative scale, therefore in the comparison with the theory they have been rescaled by a common factor. The CCC predicts correctly both the shape and the relative intensity versus  $\theta_1$  of the TDCS. The TDCS measured with the two helicities of the light are reported in the insets of figure 1(d). In these insets the TDCS measured at the three  $\theta_1$  have been added up. This procedure is strictly valid only for fully circularly polarized radiation. However in our cases neither a simulation with the CCC considering the actual characteristics of light nor the measurements of the TDCS at the three  $\theta_1$  display variations larger than the experimental uncertainties. Thus we concluded that the second term in equation (1) does not contribute significantly to the measured TDCS and therefore

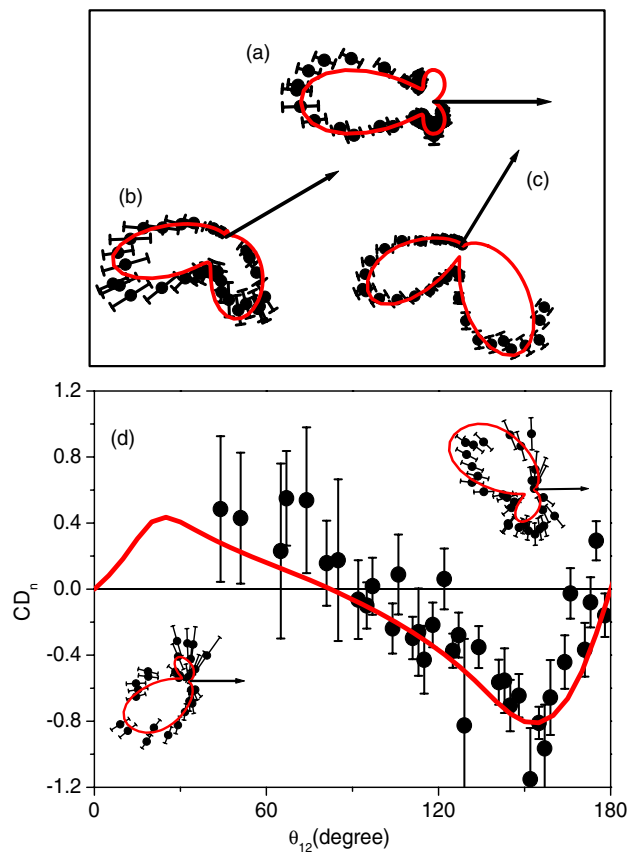


**Figure 1.** He TDCS for  $E_1 = 3.5$  eV,  $E_2 = 44.5$  eV,  $S_1 = 1$  and  $\theta_1 = 0^\circ$  (a),  $30^\circ$  (b) and  $60^\circ$  (c) with respect to the polarization axis. The  $CD_n$  versus  $\theta_{12}$  is shown in panel (d). The TDCS obtained with the two helicities of the radiation are reported in the top-right (TDCS<sub>R</sub>) and bottom-left (TDCS<sub>L</sub>) corners of the same panel. The experimental TDCS are compared with the predictions of the CCC model (solid line).

derived the  $CD_n$  (figure 1(d)) according to equation (3). A reasonable agreement between the CCC theory and experiment is observed also for the measurements with the two helicities and the  $CD_n$  (figure 1(d)).

Following the procedure by Bolognesi *et al* [5] the three independent determinations of the TDCS at the same  $E_1, E_2$  and

$\theta_{12}$  are inserted in a nonlinear system based on equation (1), whose solution gives  $|a_g|^2$ ,  $|a_u|^2$  and  $\cos \delta$ . The uncertainties in these quantities have been calculated using equations (4)–(6) of [5] under the assumption that the uncertainties in the three experimental TDCS are statistically independent. These quantities when used to reproduce the measured  $CD_n$  provide us with the sign of the relative phase  $\delta$ , too. Due to the geometrical constraints of our set-up the amplitudes and the phase are measured only in the region  $\theta_{12} > 90^\circ$ . The results are shown in figure 2, where they are compared with the CCC predictions and the previous data of [5] measured at  $h\nu = 119$  eV ( $E_1 = 5$  eV and  $E_2 = 35$  eV). Good agreement with the theoretical predictions is observed also for the shape of the amplitudes and phase measured in the two experiments. However the different  $R$  of the two sets of data results in a different  $|a_g|^2/|a_u|^2$  ratio, indeed  $|a_u|^2$  of [5] in figure 2 has been scaled up by a factor 1.6. The knowledge of  $a_g$ ,  $a_u$  and  $\delta$  allows to calculate other observables of the process. The linear dichroism,  $\Delta_{lin} = \Delta TDCS(E_1 \leftrightarrow E_2)$ , i.e. the difference between two TDCS measured with linearly polarized radiation in which the energies of the two electrons are exchanged, has been calculated at  $\theta_1 = 0^\circ$  and compared with CCC in figure 3(a). Then by integrating equation (1) over all the directions of one of the two photoelectrons [16] the asymmetry parameter,  $\beta$ , of the angular distribution of the fast (slow) photoelectron,  $d^2\sigma/dE d\Omega_i \propto 1 + \beta_i P_2(\cos \theta_i)$   $i = 1, 2$ , can be obtained. The calculated  $\beta$  ( $0.68 \pm 0.14$  and  $-0.12 \pm 0.10$  for the fast and slow photoelectron, respectively) from the present amplitudes and phase well compare with the CCC values (0.80 and  $-0.18$ , respectively). These values can be compared with previous experimental [17] and theoretical [16] values at  $h\nu = 120$  eV. At the same  $R = E_1/E_2$  ratio of the present experiment, good agreement is found for the  $\beta$  of the fast photoelectron, while the experimental value [17] of the slow photoelectron appears to be higher ( $0.5 \pm 0.2$ ). Finally also the He<sup>2+</sup> recoil momentum distribution,  $d\sigma/dK$ , where  $K = k_1 + k_2$  is the centre of mass of the two-electron subsystem and therefore the opposite of the ion recoil momentum, has been calculated [18] and compared in figure 3(b) with the predictions of CCC, because no experiments exist at this  $h\nu$ . This latter finding shows for the first time that it is possible to reconstruct from an electron–electron experiment with fixed

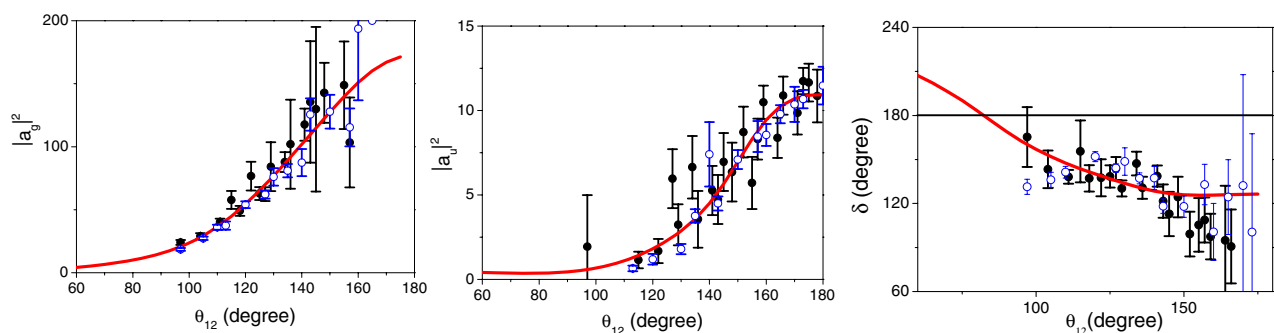


**Figure 2.**  $|a_g|^2$ ,  $|a_u|^2$  and  $\delta$  as obtained from the experimental TDCS and the  $CD_n$  shown in figure 1 are compared with the predictions of the CCC (full line) at  $h\nu = 127$  eV and with the values obtained in [5] (open circles). In the transformation from  $\cos \delta$  to  $\delta$  for the data in [5] the same sign used for the present data has been adopted. The  $|a_u|^2$  values of [5] have been rescaled by a factor 1.6 (see the text).

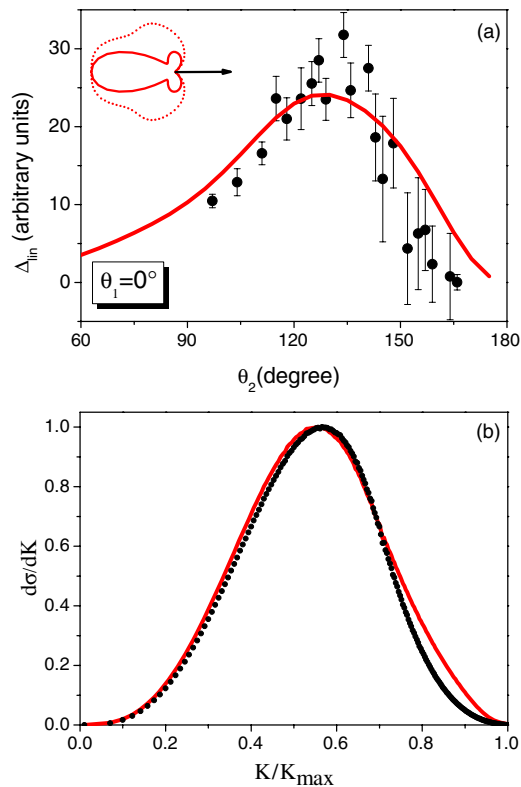


**Figure 3.** (a)  $\Delta_{\text{lin}}$  calculated from the experimental  $a_g$ ,  $a_u$  and  $\delta$  for  $\theta_1 = 0^\circ$  is compared with the CCC (full line). In the inset the complementary TDCS predicted by the CCC are reported in a polar plot:  $E_1 = 3.5$  eV,  $E_2 = 44.5$  eV and  $\theta_1 = 0^\circ$  (full line),  $E_1 = 44.5$  eV,  $E_2 = 3.5$  eV and  $\theta_1 = 0^\circ$  (dotted line); (b)  $d\sigma/dK$  versus the rescaled momentum of recoiling nucleus. The  $d\sigma/dK$  calculated from experimental amplitudes (dotted line) is compared with CCC (solid line), both curves are renormalized to a maximum value of 1.

analyzers a typical observation of a COLTRIMS experiment. None of the observables of PDI studied up to now, apart from the CD, relies on the sign of  $\delta$ . However by similarities with photoionization [19], we expect that this quantity plays a role in the determination of the spin asymmetry parameters of the two electrons of PDI.

In figure 1(d) the  $CD_n$  crosses zero at about  $\theta_{12} = 85^\circ$ . It can be easily checked in equation (3), that this is a ‘dynamic node’ due to a zero in  $\sin \delta$ . Indeed in figure 2 the theory predicts  $\delta = \pi$  at this  $\theta_{12}$ . Recently Istomin *et al* [11] predicted that ‘at all excess energies up to 50 eV’ two dynamic nodes should be observed in the ranges  $14.6^\circ \leq \theta_{12} \leq 40.1^\circ$  and  $81.3^\circ \leq \theta_{12} \leq 88.4^\circ$ . We confirm the existence of a node in the range of the larger  $\theta_{12}$ . No experimental data cover the other range, however our calculations do not support the prediction of a node in that region. To investigate better the existence of dynamic nodes other measurements have been done at  $102.5 \leq h\nu \leq 142.5$  eV.  $E_1$  was kept at 3.5 eV, while  $E_2$  was incremented according to the variation of  $h\nu$ . In figure 4(a) the  $CD_n$  measured at six  $E_2$  is reported versus  $\theta_{12}$ . While a change in sign of the  $CD_n$  at certain  $E_2$  values is observed for  $\theta_{12} < 127^\circ$ , in the measurements at  $\theta_{12} \geq 127^\circ$  all the measured  $CD_n$  are negative. To emphasize this result the  $CD_n$  at  $\theta_{12} = 67^\circ$ ,  $97^\circ$  and  $127^\circ$  is reported versus

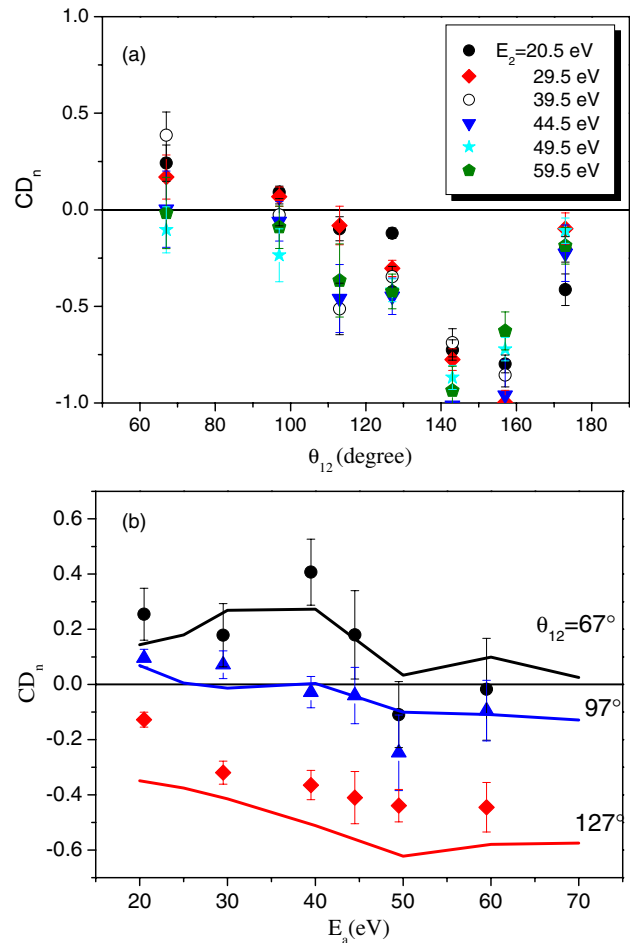


**Figure 4.**  $CD_n$  versus  $\theta_{12}$  at  $E_1 = 3.5$  eV and six different  $20.5 \leq E_2 \leq 59.5$  eV (a) and versus  $E_2$  at  $\theta_{12} = 67^\circ$  (dots),  $97^\circ$  (triangle) and  $127^\circ$  (diamond) (b). The solid lines in (b) are the CCC predictions. The data at  $E_2 = 44.5$  eV are the weighted average of the  $CD_n$  obtained in this measurement and the one from the measurement of the full TDCS shown in figure 1(d).

$E_2$  in figure 4(b). Consistently with the CCC predictions the  $CD_n$  changes sign at  $\theta_{12} = 97^\circ$  when  $E_1 = 3.5$  eV and  $E_2 \approx 35$  eV. This definitely proves the existence of the dynamic nodes, whose occurrence depends on  $E_1/E_2$  and  $\theta_{12}$ , as firstly predicted by Berakdar *et al* [7]. From equation (2) it is evident that the appearance of a dynamic node corresponds to the mathematical condition of linear dependence of the two amplitudes. This results in a reduction of the dimensionality of the process. Dichroism is intrinsically a 3D phenomenon, thus the  $(E_1, E_2, \theta_{12})$  sets with  $\delta = 0, \pi$  correspond to dynamic conditions where the PDI process loses in a non-trivial way its 3D characteristics.

The achievement of complete experiments is one of the main goal in atomic physics. Photoelectron-Auger electron [20] and photoelectron-ion [21] coincidence experiments have been proved to be an ideal tool for complete photoionization experiments. Here electron–electron coincidence experiments with linearly and circularly polarized radiation enabled us to obtain the determination of the amplitudes needed for a complete quantummechanical description of the PDI in

He. It has been shown that the data measured with fixed analyzers can be used to determine the  $\text{He}^{2+}$  momentum distribution, a typical result of COLTRIMS. Another result is the observation of a node in the CD when the relative phase between the two amplitudes is  $\pi$ . Analytical methods [22] showed that the vanishing of CD at certain  $(E_1, E_2, \theta_{12})$  is completely dependent on electron correlations and the position of the dynamic nodes varies depending on the used wavefunctions [7]. The definite prove of their existence and their clear identification in the multidimensional  $(E_1, E_2, \theta_{12})$  space may be used to discriminate among different correlated wavefunctions and may be of prominent importance in the understanding of one-photon two-electron emission in highly correlated materials [23]. The existence of dynamic nodes has been also correlated to a non-trivial reduction of dimensionality of the process.

### Acknowledgments

Work partially supported by INTAS Project No 0–51-4706, MIUR FIRB project ‘Probing the microscopic dynamics of chemical reactivity’. V F thanks the ICTP for a TRIL scholarship and A K for the CNR-Short Term Mobility program.

### References

- [1] Avaldi L and Huetz A 2005 *J. Phys. B: At. Mol. Opt. Phys.* **38** S861
- [2] Huetz A, Selles P, Waymel D and Mazeau J 1991 *J. Phys. B: At. Mol. Opt. Phys.* **24** 1917
- [3] Malegat L, Selles P and Huetz H 1997 *J. Phys. B: At. Mol. Opt. Phys.* **30** 251
- [4] Cvejanovic S and Reddish T 2000 *J. Phys. B: At. Mol. Opt. Phys.* **33** 4691
- [5] Bolognesi P, Kheifets A S, Bray I, Malegat L, Selles P, Kazansky A K and Avaldi L 2003 *J. Phys. B: At. Mol. Opt. Phys.* **36** L241
- [6] Berakdar J and Klar H 1992 *Phys. Rev. Lett.* **69** 1175
- [7] Berakdar J and Klar H 2001 *Phys. Rep.* **340** 473
- [8] Berakdar J, Klar H, Huetz A and Selles P 1993 *J. Phys. B: At. Mol. Opt. Phys.* **26** 1463
- [9] Krässig B 2001 Correlations, polarization and ionization in atomic systems *AIP Conf. Proc.* 604 (Rolla, USA) ed D H Madison and M Schulz p 12
- [10] Knapp A *et al* 2005 *J. Phys. B: At. Mol. Opt. Phys.* **38** 645
- [11] Kheifets A S and Bray I 1998 *J. Phys. B: At. Mol. Opt. Phys.* **31** L447
- [12] Kheifets A S and Bray I 1998 *Phys. Rev. Lett.* **81** 4588
- [13] Istomin A Y, Manakov N L and Starace A F 2004 *Phys. Rev. A* **69** 32713
- [14] Collins S A *et al* 2002 *Phys. Rev. A* **65** 052717
- [15] Bolognesi P, Coreno M, Alberti G, Richter R, Sankari R and Avaldi L 2004 *J. Electron. Spectrosc. Relat. Phenom.* **141** 105
- [16] Blyth R R *et al* 1999 *J. Electron Spectrosc. Relat. Phenom.* **101–3** 959
- [17] Desiderio D *et al* 1999 *Synchrotron Radiat. News* **12** 34
- [18] Proulx D and Shakeshaft R 1993 *Phys. Rev. A* **48** R875 (see also [15] in this paper)
- [19] Whelitz R, Heiser F, Hemmers O, Langer B, Menzel A and Becker U 1991 *Phys. Rev. Lett.* **67** 3764
- [20] Pont M and Shakeshaft R 1996 *Phys. Rev. A* **50** 1448
- [21] Huang K-N 1980 *Phys. Rev. A* **22** 223
- [22] Bolognesi P, De Fanis A, Coreno M and Avaldi L 2004 *Phys. Rev. A* **70** 22701
- [23] Shigemasa E, Adachi J, Soejima K, Watanabe N, Yagishita A and Cherepkov N A 1998 *Phys. Rev. Lett.* **80** 1622
- [24] Berakdar J 1998 *J. Phys. B: At. Mol. Opt. Phys.* **31** 3167
- [25] Hermann R, Samarin S, Schwabe H and Kirschner J 1998 *Phys. Rev. Lett.* **81** 2148